ELSEVIER

Journal of Crystal Growth 204 (1999) 293–297

JOURNAL OF CRYSTAL GROWTH

www.elsevier.nl/locate/jcrysgro

Structural characteristics of *a*-axis-oriented $PrBa_2Cu_3O_7$ thin films grown by pulsed laser deposition

Rong-ping Wang[a,*], Yue-liang Zhou[a], Shao-hua Pan[a], Huan-hua Wang[a], Guo-zhen Yang[a], Guang-wen Zhou[b], Ze Zhang[b]

[a]*Laboratory of Optical Physics, Institute of Physics & Center for Condensed Matter Physics, Chinese Academy of Sciences, Beijing 100080, People's Republic of China*

[b]*Beijing Laboratory of Electron Microscopy, Center for Condensed Matter Physics, Chinese Academy of Sciences, Beijing 100080, People's Republic of China*

Received 12 March 1999; accepted 15 March 1999
Communicated by M. Schieber

Abstract

PBCO films have been successfully fabricated at different temperatures. X-ray diffraction results show that the orientation of PBCO films varies with decreasing deposition temperature. The optimal deposition condition for *a*-axis oriented PBCO films is 15 Pa oxygen pressure and 700°C. Raman scattering measurements indicate that the 514 cm^{-1} of A_g phonon mode can be used as a criterion for determining whether the film is *a*-axis-oriented or not, e.g., the intensity of 514 cm^{-1} mode is the strongest for *c*-axis-oriented film but almost disappears for *a*-oriented film. High-resolution transmission electron microscopy confirms that our *a*-axis-oriented film has a good structural quality.

PACS: 68.55; 81.15.F; 07.85.N; 78.30; 61.16.B

Keywords: PBCO film; Pulsed laser deposition; XRD; Raman spectroscopy; TEM

1. Introduction

One of the most promising applications of the high-temperature superconducting (HTSC) $YBa_2Cu_3O_{7-\delta}$ (YBCO) films is to fabricate Josephson junctions having both uniform critical current density (J_c) and normal resistance (R_n). It has been well known that the coherent length, ξ_{ab}, in the *a*- and *b*-axis directions laying in the copper-oxide planes is much larger than, ξ_c, normal to the copper-oxide planes. Hence it is desired to fabricate HTSC films with a crystal orientation that presents the edges of the CuO_2 planes at the surface of the film in order to take advantage of the larger coherence length along this direction. The simple way to prepare *a*-axis-oriented YBCO films is to lower the deposition temperature by roughly 100°C from that used to grow *c*-axis film. Unfortunately, high-quality *a*-axis YBCO films are generally difficult to prepare than standard *c*-axis films. In general, *a*-axis-oriented film has much smaller grains than *c*-axis film, resulting in a

* Corresponding author.
E-mail address: xyw@aphy.iphy.ac.cn (R.-p. Wang)

0022-0248/99/$ - see front matter
PII: S0022-0248(99)00176-1

rougher surface. In addition, the *a*-axis-oriented film contains *b*/*c* twin boundaries, these twin boundaries can seriously limit J_c of the films [1–6]. Recently, intense attention has been paid to $PrBa_2Cu_3O_7$ (PBCO) because of its perplexing anomaly in contrast with almost all other "123" stoichiometry (R) $Ba_2Cu_3O_7$, where R is a rare-earth element. Nearly, all (R) $Ba_2Cu_3O_7$ are superconductors having a T_c near 90 K, with the notable exception of PBCO. It has been found that the resistivity of PBCO showed nonmetallic hopping characteristics commonly associated with an underdoped semiconductor. Due to structural similarity with its superconducting relatives but apparently nonmetallic, PBCO is a natural choice as an epitaxial barrier material in HTSC devices [7]. An ordered crystalline in PBCO thin films will be beneficial to the epitaxial growth of overlayers (such as YBCO films) for Josephson weak-link fabrication. Hence, it is important to fabricate and characterize *a*-axis-oriented PBCO films.

In this paper, we report the effect of growth temperature on the preferential orientation of PBCO films on (0 0 1)$SrTiO_3$ (STO) substrates. X-ray diffraction (XRD) pattern shows that the preferential orientation changes from mixing, *a*- to *c*-orientation with increasing growth temperature. However, due to the very close lattice match between our substrate and the film, the *a*- and *b*-axis-oriented diffraction peaks are difficult to separate from the very strong substrate peaks. Therefore, in order to verify unambiguously that we indeed have the desired *a*-axis growth, we have turned to Raman scattering and transmission electron microscopy. The Raman experimental results indicate that the intensity of 514 cm^{-1} phonon mode can be used as a criterion for film orientation. High-resolution transmission electron microscopy (HRTEM) and electron diffraction (ED) patterns show that PBCO film grown at 700°C and 15 Pa oxygen pressure has nearly complete *a*-axis orientation with few *ab* twinning domains.

2. Experimental procedure

The films were fabricated by pulsed laser deposition on STO (0 0 1) substrates using a PBCO ceramic target. The substrates were polished and rinsed in organic solvents and de-ionized water before they were put into the deposition chamber. A 308 nm XeCl excimer laser-generated energy of 100 mJ/pulse on the target with a repetition rate of 3 Hz. The distance from the target to substrate was 4 cm, and the substrate temperature could be raised to appropriate values by a heater on which the substrates were mounted. During all deposition processes, the deposition chamber was prepumped to 2×10^{-3} Pa, and then O_2 was introduced at 15 Pa. The deposition time is 15 min, and the deposition temperatures are from 600 to 850°C. After deposition was completed, the films were in situ annealed at 500°C and 1 atm of oxygen for 20 min, and then cooled to room temperature. These as-grown PBCO films with thickness of 2500 Å were investigated by XRD, Raman scattering and HRTEM. A standard θ–2θ technique was employed for the crystallographic phase analysis and detection of the preferential orientation of the deposited films. By using Cu K_α radiation, the diffracted intensity and the full-width at half-maximum (FWHM) were recorded at 0.02° intervals over a range of 20–60°. The Raman scattering measurements were performed using a Spex 1403 photomultiplier equipped with photocounting system. A spectra-Physics 171 Argon ion laser with a 488 nm line served as the excitation source at an incident power of 10 mW on sample with incident angle of 15°. The polarization of the incident beam was parallel to the surface of the film and the scattered light was collected at backscattering geometry with no polarization analysis of the outgoing radiation. The instrumental resolution was 2 cm^{-1}. HRTEM and ED investigations were performed on a JEOL-2010 operating at 200 kV with point-to-point resolution of 1.94 Å. Cross-section sample for TEM was mechanically polished to a thickness of 15 μm, and then further thinning with Ar ion milling using standard procedure.

3. Results and discussion

As mentioned above, it is difficult to determine the orientation of film from XRD because of the very close lattic match. In the vicinity of four peaks

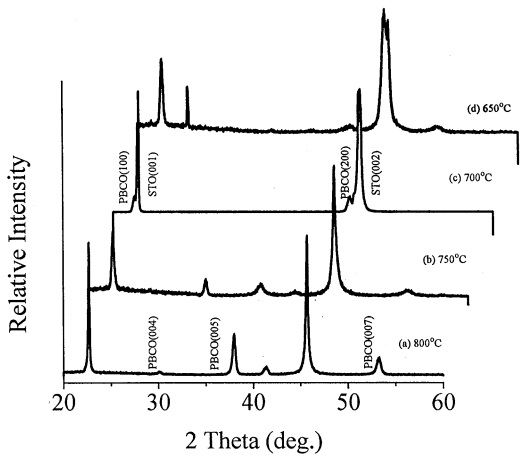

Fig. 1. XRD patterns of PBCO films deposited at various temperatures.

of (0 0 L) STO substrate, the corresponding a, b, c-oriented diffraction peaks of PBCO overlay with substrate peaks. However, we can use weak (0 0 5) peak as a criterion because it is the strongest peak representing c-axis-oriented film apart from those (0 0 L) peaks of PBCO which overlap with substrate peaks. In other words, if XRD result shows (0 0 5) peak, we can at least partly conclude that the film contains c-axis-oriented grain, while if no (0 0 5) peak, it suggests that the film is a- or b-axis orientation dominant. Fig. 1 shows the typical XRD results of the PBCO films deposited at different temperatures. It can be seen that, highly crystalline c-axis-oriented films can be prepared at 800°C as shown in Fig. 2a. The quality of crystalline alignment degrades with decreasing growth temperature, but then it recovers and again approaches the best quality for a-axis-oriented growth near 700°C as shown in Fig. 2c, where the film displays nearly complete a-axis orientation. The a-axis-oriented film can be determined according to the procedure as follows: No (0 0 5) peak existing in Fig. 1c suggests that the film is a- or b-axis-oriented dominant as stated above. On the other hand, the lattice constants of a and b in PBCO are respectively 3.918 and 3.901 Å [8] and that of cubic STO is 3.905 Å. The 2θ value of corresponding diffraction peak should be smaller for a-axis-oriented film but greater for b-axis-oriented film compared with that of corresponding substrate peaks. Obviously, in Fig. 1c, a weak shoulder exists in the left of each (0 0 L) STO substrate peak, so we can conclude that the film grown at 700°C is nearly complete a-axis orientation.

In two considerable wide temperature ranges from 600 to 670°C and from 720 to 780°C, the as-grown films show a mixing a- and c-orientation, which are in good agreement with Refs. [2,4]. In addition, a weak peak at $2\theta = 41.78^\circ$ can be seen in Figs. 1a–d. In early work, this peak was ascribed to impurity phase of $BaCuO_2$; this impurity phase still existed even at their best quality a-axis-oriented film. However, no impurity exists for our a-axis orientation film as shown in Fig. 1c, indicating that our a-axis-oriented film is of high quality.

To further confirm our XRD results, Raman spectrum was used to characterize the film orientation. Fig. 2 shows the room-temperature Raman spectra of our a- and c-axis-oriented films and their decomposition into several Lorentzians. The Raman spectrum of the c-axis-oriented film has three features at 296, 421 and 514 cm^{-1}, which have been assigned to the A_g vibration modes of

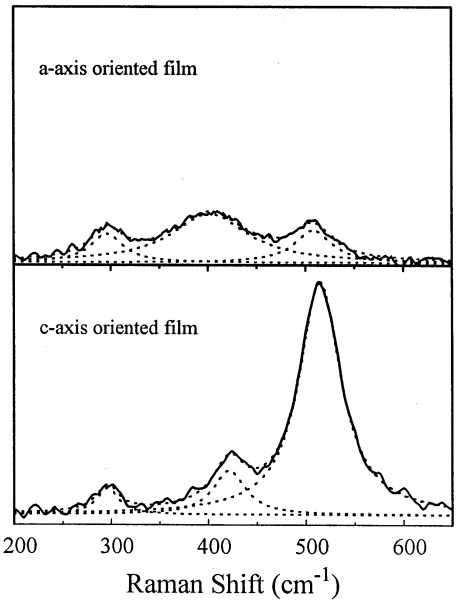

Fig. 2. Raman spectra for a- and c-axis-oriented films, the ordinates for the upper and lower figures have the same scale.

Table 1
Peak positions and their scattering intensities for *a*- and *c*-axis-oriented films

a-axis-oriented film		*c*-axis-oriented film	
Peak	Intensity	Peak	Intensity
296	3546	296	2260
401	14 183	421	5593
507	4617	514	37 871

O(2,3) out-of-phase, in-phase bending and O(4)-bridging oxygen stretching, respectively [9–11]. The Raman spectrum of the *a*-axis-oriented film shows three peaks at 296, 401 and 507 cm^{-1}. Table 1 lists the peak positions and their scattering intensities for *a*- and *c*-axis-oriented films based on the results from decomposing Raman spectra into several Lorentzians. Two obvious features can be found: in-phase bending mode downshifts from 421 cm^{-1} for *c*-axis-oriented film to 401 cm^{-1} for *a*-axis-oriented film, and the scattering intensity of O(4)-bridging oxygen stretching mode shows remarkable decrease from *c*- to *a*-axis-oriented film. For the former, Rosen et al. [9] proposed that the strain effect and oxygen deficiency are possible reasons. Due to the very close lattice match in the as-grown films, Raman shift caused by the strain effect is less than 5 cm^{-1}, suggesting that the strain effect is not enough to explain Raman shift, and the other possible reason due to the disorder induced by oxygen deficiency should be considered. Our detailed X-ray photoelectron spectroscopy investigation confirms that oxygen content of the film deposited at high temperature is larger than that at low temperature [12]. Early results [13,14] showed that oxygen content has a significant effect on the frequency of the phonon mode, e.g., the frequency of O(4) bridging oxygen modes decreases but that of O(2,3) in-phase bond bending mode increases with decreasing oxygen content. This conclusion is in contradiction with our experimental results, and suggests that the other mechanism must be considered to explain these Raman shifts.

In our Raman scattering experiments, experimental geometry is the same for *a*- and *c*-axis-oriented film, both incident and scattering lights are at a small angle with the normal of the surface of the films, strikingly speaking, all of our obtained modes are oblique phonons; moreover, the variation of the film orientation will result in significant phonon directional dispersion, and hence the variation of vibrational frequency. From the calculated phonon dispersion curves of YBCO [15], the O(2,3) out-of-phase bond bending and O(4) bridging oxygen stretching shows slightly directional dispersion while that of in-phase bond bending being about 30 cm^{-1} dispersion. By comparison with the phonon dispersion curve of YBCO, the Raman shift for PBCO films can be reasonably explained.

Raman scattering intensity of O(4) bridging oxygen stretching can be used as a criterion for film orientation. This mode was found to be the strongest mode in a single crystal if the $\boldsymbol{E}$ vector was perpendicular to the *a–b* plane but disappeared if the $\boldsymbol{E}$ vector was along the *a–b* plane. Again, due to the paraxial character of the incident and scattering light, it is impossible to disappear completely for the O(4) bridging oxygen stretching mode. Combined with our experimental geometry, the remarkable decrease of the Raman scattering intensity of O(4) bridging oxygen stretching can be considered intrinsically for *a*-axis film in our experimental geometry. Further, polarized Raman scattering experiments may be more obvious to show that E_g vibrational modes can also be used as a criterion for film orientation.

The cross-sectional overview indicates, in considerable wide observed regions that the PBCO film grown at 700°C and 15 Pa oxygen pressure is *a*-axis oriented. Fig. 3a shows the typical cross-sectional HRTEM image of PBCO/STO. The interface is atom sharp and no secondary phase is found, and the perovsike mesh is continued across the interface. The inset in Fig. 3a is the corresponding ED pattern. According to the HRTEM observation, domains showing an *ac* twinning could scarcely be detected, well in agreement with our results obtained from XRD and Raman spectroscopy. However, few *ab* twinning domains have also been observed as shown in Fig. 3b, this kind of defect structure is insensitive to XRD and Raman spectroscopy.

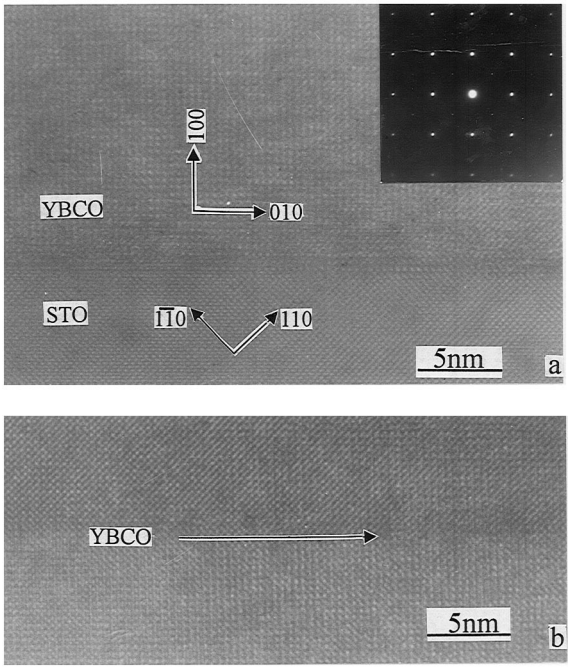

Fig. 3. [1 0 0] cross-sectional HRTEM images of *a*-axis-oriented PBCO film grown on $SrTiO_3$ (0 0 1) substrate, the electron beam is parallel to [0 0 1]. (a) The typical perfect interface which shows the orientation relationship between the PBCO film and $SrTiO_3$ substrate, the inset is the corresponding ED pattern, (b) *ab* twinning domain.

4. Conclusions

We report the effect of growth temperature on the preferential orientation of PBCO films on (0 0 1) STO substrates in this article. XRD pattern shows that the preferential orientation changes from mixing, *a*- to *c*-orientation with increasing growth temperature, and the optimal growth condition for *a*-axis-oriented PBCO film is 700°C and 15 Pa oxygen pressure. Comparing Raman spectrum of *a*-axis-oriented film with that of *c*-axis-oriented film, we conclude that the intensity of 514 cm^{-1} can be used as a criterion for film orientation. HRTEM and ED pattern show that PBCO film grown at 700°C and 15 Pa oxygen is nearly complete *a*-axis orientation with few *ab* twinning domains.

References

[1] T. Venkatesan, A. Inam, B. Dutta, R. Ramesh, M.S. Hegde, X.D. Wu, L. Nazar, C.C. Chang, J.B. Barner, D.M. Hwang, C.T. Rogers, Appl. Phys. Lett. 56 (1990) 391.
[2] M. Inam, C.T. Rogers, R. Ramesh, K. Remschning, L. Farrow, D. Hart, T. Venkatesan, B. Wikens, Appl. Phys. Lett. 57 (1990) 2484.
[3] J.B. Barner, C.T. Rogers, A. Inam, R. Ramesh, S. Bersey, Appl. Phys. Lett. 59 (1991) 742.
[4] M. Mukaida, S. Miyazawa, J. Appl. Phys. 74 (1993) 1209.
[5] Z. Trajanovic, I. Takeuchi, P.A. Warbarton, C.J. Lobb, T. Venkatesan, Appl. Phys. Lett. 66 (1995) 1536.
[6] I. Takeuchi, P.A. Warbarton, Z. Trajanovic, C.J. Lobb, Z.W. Dong, T. Venkatesan, M.A. Bari, W.E. Booij, E.J. Tarte, M.G. Blamire, Appl. Phys. Lett. 69 (1996) 112.
[7] M. Lee, M.L. Statzman, Y. Suzuki, T.H. Geballe, Phys. Rev. B 54 (1996) R3776.
[8] K. Weishaupt, J.Th. Held, H.D. Hochhelmer, S.B. Qudri, E.F. Skelton, K. Brister, J. Phys. Chem. Solids 59 (1998) 211.
[9] M.J. Rosen, R.M. Macfarlane, E.M. Engler, V.Y. Lee, R.D. Jacowitz, Phys. Rev. B 38 (1988) 2460.
[10] M. Cardona, in: S.K. Joshi, C.N.R. Rao, S.V. Subramanyam (Eds.), International Conference on Superconductivity, World Scientific, Singapore, 1990.
[11] N. Watanabe, K. Kuroda, K. Abe, N. Koshizuka, M. Tagami, Y. Shiohara, Physica C 300 (1998) 301.
[12] Rong-ping, Wang, Shao-hua Pan, Yue-liang Zhou, Appl. Surf. Sci., submitted.
[13] Y. Liu, G. Pandlinan, R. Soorgakumar, J. Summer, T. Lemberger, J. Appl. Phys. 64 (1988) 3598.
[14] L.A. Farrow, S.-W. Chan, L. Greene, W. Feldmqnu, J. Appl. Phys. 65 (1989) 2381.
[15] W. Kress, U. Schroder, J. Prade, A.D. Kulkarni, F.W. de Wette, Phys. Rev. B 38 (1988) 2906.